Current Biology, Vol. 14, 697–703, April 20, 2004, ©2004 Elsevier Ltd. All rights reserved. DOI 10.1016/j.cub.2004.04.008

Imaging Sites of N-WASP Activity in Lamellipodia and Invadopodia of Carcinoma Cells

Mike Lorenz,* Hideki Yamaguchi, Yarong Wang, Robert H. Singer, and John Condeelis
Albert Einstein College of Medicine
Department of Anatomy and Structural Biology
1300 Morris Park Avenue
Bronx, New York 10461

Summary

Cell migration is crucial for many biological and pathological processes such as chemotaxis of immune cells, fibroblast migration during wound healing, and tumor cell invasion and metastasis. Cells migrate forward by extending membrane protrusions. The formation of these protrusions is driven by assembly of actin filaments at the leading edge [1]. Neural Wiskott-Aldrich syndrome protein (N-WASP), a ubiquitous member of the WASP family, induces actin polymerization by activating Arp2/3 complex and is thought to regulate the formation of membrane protrusions [2, 3]. However, it is totally unclear how N-WASP activity is spatially and temporally regulated inside migrating cells. To detect and image sites of N-WASP activity during cell motility and invasion in carcinoma cells, we designed an N-WASP fluorescence resonance energy transfer (FRET) biosensor that distinguishes between the active and inactive conformations and mimics the function of endogenous N-WASP. Our data show that N-WASP is involved in lamellipodia extension, where it is activated at the leading edge, as well as in invadopodia formation of invasive carcinoma cells, where it is activated at the base. This is the first time that the activity of full-length N-WASP has been visualized in vivo, and this has lead to new insights for N-WASP function.

Results and Discussion

N-WASP is a central regulator of the actin cytoskeleton. Biochemical studies have revealed that several signaling molecules, including Cdc42, WISH, WIP, Grb2, phosphoinositides, and Src-family kinases, activate N-WASP to bind Arp2/3 complex at its C-terminal VCA domain (verprolin homology, cofiling homology, and acidic region) (for a review see [4]). The activity of N-WASP is believed to be regulated by an intramolecular interaction between the VCA domain and an N-terminal regulatory region thereby forming an autoinhibitory folded conformation [5, 6] (see Figure 1A). However, the spatial and temporal regulation of N-WASP in cells is not known. Based on the postulated self-regulation of N-WASP [5] and the autoinhibitory conformation of WASP [6], we designed a biosensor that exhibited intramolecular fluorescence resonance energy transfer (FRET) between cyan fluorescent protein (CFP) and yellow fluorescent protein (YFP) fused to the N or C termini of N-WASP, respectively (Figure 1A). In the absence of regulatory binding partners, e.g., the Rho family GTPase Cdc42, the closed, autoinhibited, inactive conformation should allow an energy transfer from the N-terminal CFP to the C-terminal YFP. Activation of N-WASP releases the VCA domain and leads to a conformational change [5, 6], increasing the CFP-YFP distance and resulting in a decreased FRET signal that allows detection, both temporally and spatially, of the activity of N-WASP in vivo.

To confirm that our N-WASP biosensor (N-WASP-BS) showed an energy transfer in vivo, we expressed the biosensor in HEK293 cells and determined the FRET efficiency by acceptor photobleaching experiments (Figure 1B). The CFP signal was imaged before and after photobleaching of YFP in the marked regions in Figure 1B (see also Figure S1). The CFP fluorescence intensity increased in the photobleached areas, indicating FRET. The FRET efficiency of the inactive N-WASP conformation was 19% $\pm$ 2%, corresponding to a CFP-YFP distance of approximately 6.3 nm. To confirm a conformational change after activation of the N-WASP-BS, we measured fluorescence emission spectra of HEK293 cell lysates expressing the N-WASP-BS in the presence and absence of constitutively active Cdc42 (L61Cdc42), dominant-negative Cdc42 (N17Cdc42), or Rac1 (L61Rac1) (Figure 1C). Due to FRET in the inactive conformation of the biosensor, two emission peaks at 474 nm (CFP) and 525 nm (YFP) were observed upon excitation at 434 nm. In presence of activated Cdc42, the CFP emission at 474 nm increased, while the YFP emission at 525 nm decreased. In the case of dominant-negative Cdc42 or Rac1, no change was observed, indicative of a conformational change induced only by Cdc42-GTP (Figure 1C). In addition activation of N-WASP by WISH, another known activator binding to the proline-rich domain of N-WASP [7], leads also to a conformational change of N-WASP-BS (see Figure S2).

The decrease in FRET after N-WASP activation by Cdc42 and WISH is consistent with two possible mechanisms: (1) an intramolecular autoinhibition, where the C-terminal VCA domain binds to an N-terminal regulatory region [5, 6], or (2) an intermolecular head-to-tail dimerization of N-WASP [8, 9]. To determine which interaction was occurring, we coexpressed the N-WASP-BS and a V5-His-tagged N-WASP and immunoprecipitated with either anti-GFP- or anti-V5-antibodies, respectively (see Figure S3). No coprecipitation was observed, suggesting an intramolecular regulation of N-WASP.

We then characterized the ability of the N-WASP-BS to stimulate Arp2/3-mediated actin nucleation in vitro (Figure 1D). In this assay we chose conditions where N-WASP was completely activated to determine if the C-terminal YFP tag inhibits the accessibility of the VCA compared to wt N-WASP. Equal amounts of N-WASP-BS and purified N-WASP (15 nM) induced actin nucleation with the same nucleation rate, while cell lysates from cells not expressing the N-WASP biosensor had no effect. Thus, the fluorescent tags did not interfere

*Correspondence: mlorenz@aecom.yu.edu

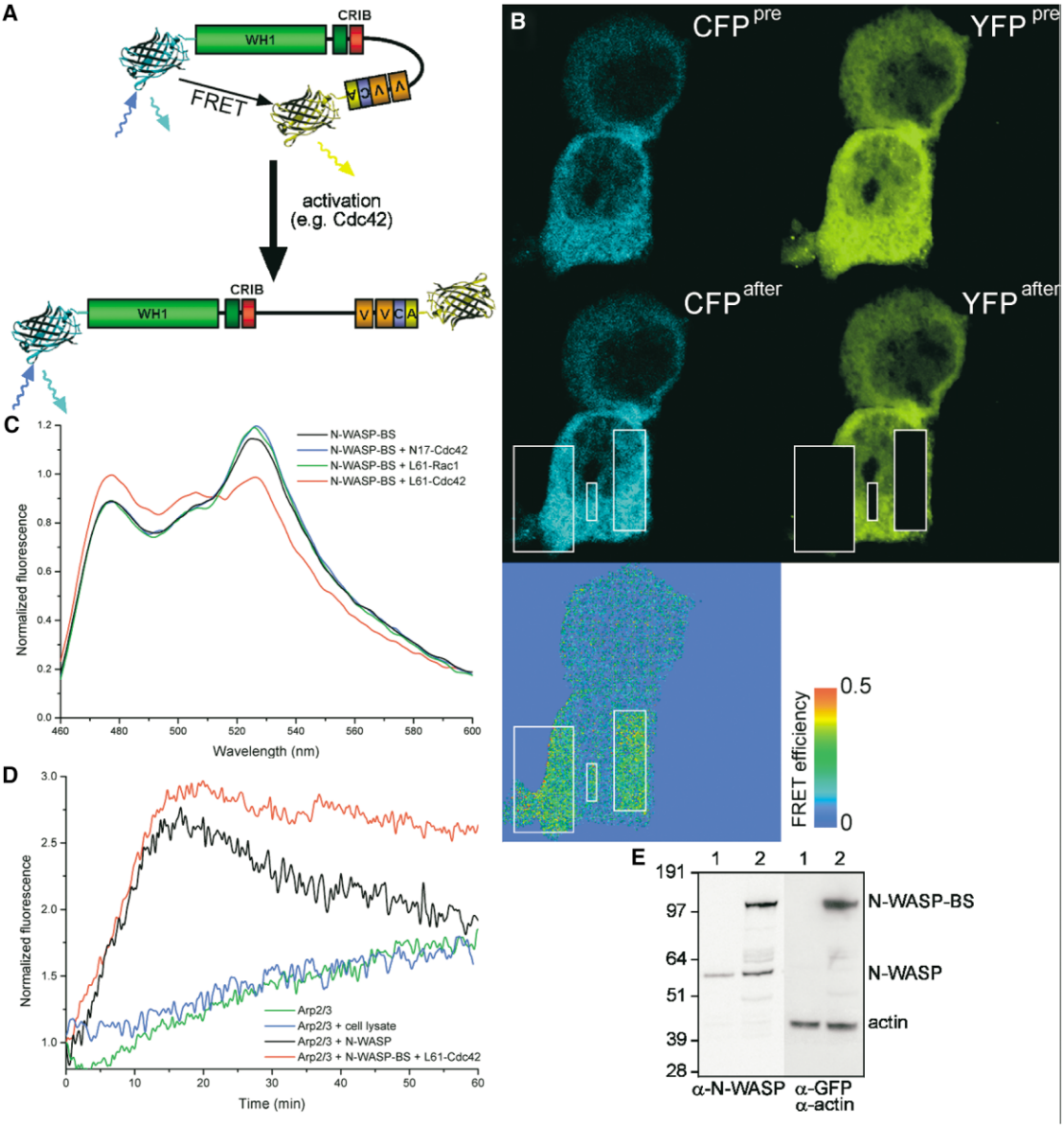

Figure 1. Generation of an N-WASP Biosensor

(A) Scheme of the N-WASP FRET biosensor. In the closed, inactive conformation of N-WASP, the N-terminal CFP and C-terminal YFP are in close proximity within nanometer range and FRET takes place. After activation by e.g., Cdc42, WISH, etc., the N-WASP conformation opens and the CFP-YFP distance increases, resulting in a loss of the FRET signal.

(B) FRET measurements by acceptor photobleaching confirmed an energy transfer in the closed conformation of the N-WASP-BS in vivo. CFP and YFP emission signals were collected before (top) and after YFP photobleaching in the marked regions (middle). In the bottom panel, the FRET efficiency E calculated for each pixel from the increase of the donor fluorescence ($E = 1 - CFP^{pre}/CFP^{after}$) is shown and is 19% ± 2% corresponding to a dye-to-dye distance of 6.3 nm.

(C) Conformational change of the N-WASP-BS after binding of Cdc42. The fluorescence spectra of ~100 nM N-WASP-BS containing cell lysates were measured in the presence (red) and absence (black) of 3 μM constitutively active Cdc42. The CFP fluorescence peak at 474 nm increased, while the YFP peak at 525 nm decreased after addition of Cdc42, indicating a conformational change in vitro, while dominant-negative Cdc42 (blue) or Rac1 (green) had no effect.

(D) N-WASP-BS increases actin nucleation. Cell lysate of N-WASP-BS and constitutively active Cdc42 coexpressing cells (red) were added to 2 μM actin containing 15% pyrene labeled actin and 27 nM purified Arp2/3 complex. The final N-WASP-BS concentration was 15 nM and the pyrene fluorescence was detected during nucleation. As a control, 15 nM purified N-WASP (black), no N-WASP (green), or lysate from nontransfected cells (blue) was added.

(E) Western blot of wt (1) and N-WASP biosensor expressing MTLn3 cells (2). The biosensor appears as a single band with the predicted molecular weight of 110 kDa and exhibits no degradation. The expression of N-WASP-BS is approximately 1.8 times above endogenous N-WASP in stable N-WASP-BS expressing MTLn3 cell lines.

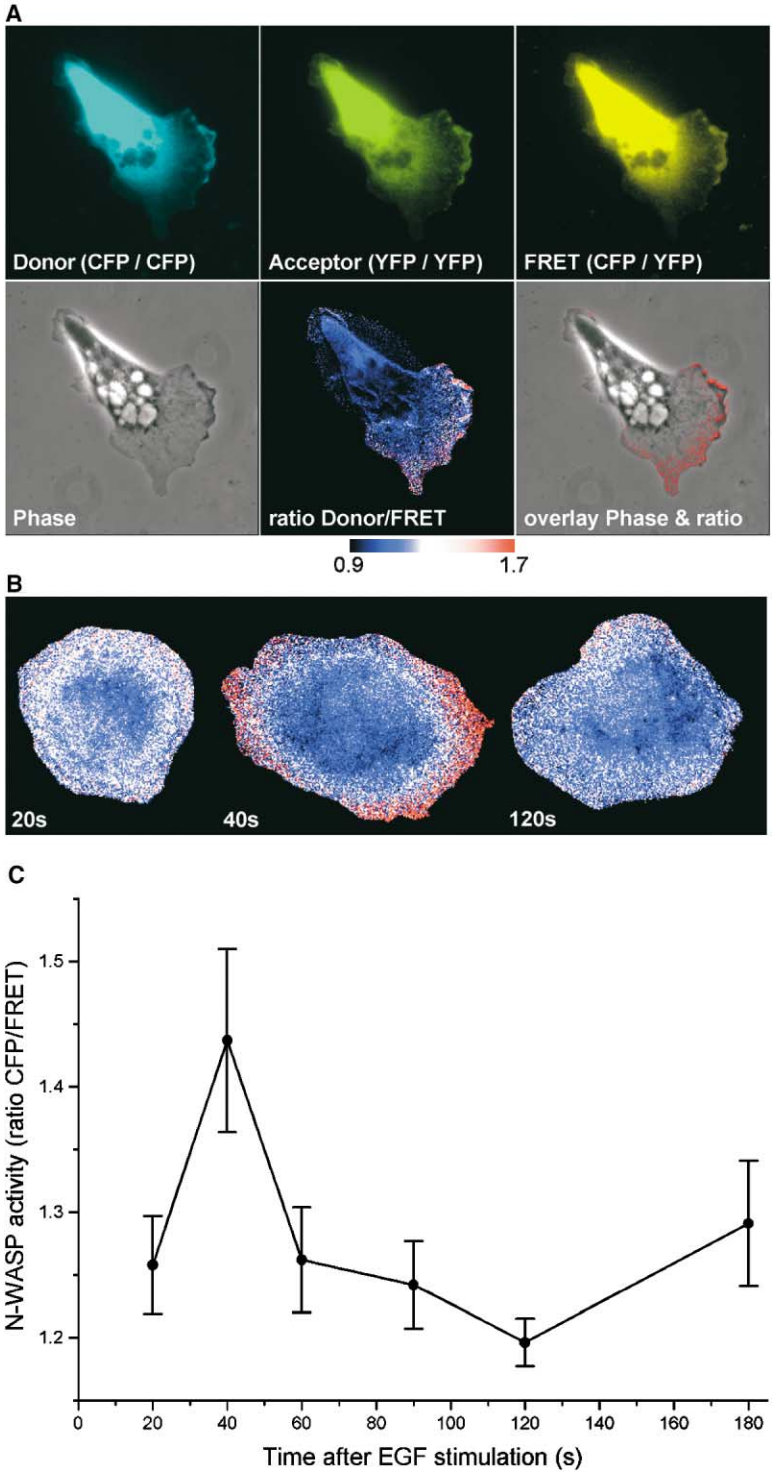

Figure 2. N-WASP Is Transiently Activated at the Leading Edge of Migrating Carcinoma Cells

(A) FRET measurements to detect the N-WASP activity in MTLn3 carcinoma cells in serum showed an N-WASP activity at the leading edge. Top row: donor (CFP), acceptor (YFP), and FRET fluorescence images (in parentheses the excitation and emission filters used are indicated); bottom row: phase image, calculated activity profile of N-WASP, and overlay with the phase image. The loss of FRET due to an activation of N-WASP was detected by rationing the donor and FRET image. The ratio increased from 1.0 in the inactive state (blue) to 1.7 for the open active conformation (red).

(B) Cells stably expressing N-WASP-BS were serum starved for 3 hr, stimulated with 5 nM EGF at 37°C, and fixed at given time points. The N-WASP activity increased at the leading edge after EGF stimulation.

(C) Kinetic measurements showed a maximum activity at the leading edge at 40 s after stimulation, a time that corresponds to the earliest actin polymerization transient in EGF stimulated cells [10]; error bars are standard deviations.

with either the activation pathway or the actin nucleation stimulating ability of N-WASP. The N-WASP-BS behaves like wt N-WASP and allows discrimination of the closed, inactive from the open, active conformation by FRET.

To detect the spatial regulation of N-WASP in migrating cells, we transfected the N-WASP-BS into MTLn3 carcinoma cells and measured its activation by FRET microscopy (Figure 2A). The FRET ratio signal calculated as the CFP fluorescence (donor image) divided by the YFP emission upon CFP excitation (FRET image) increased significantly by 1.7-fold after N-WASP activation. In motile MTLn3 cells, N-WASP activity was observed at the leading edge of lamellipodia toward the

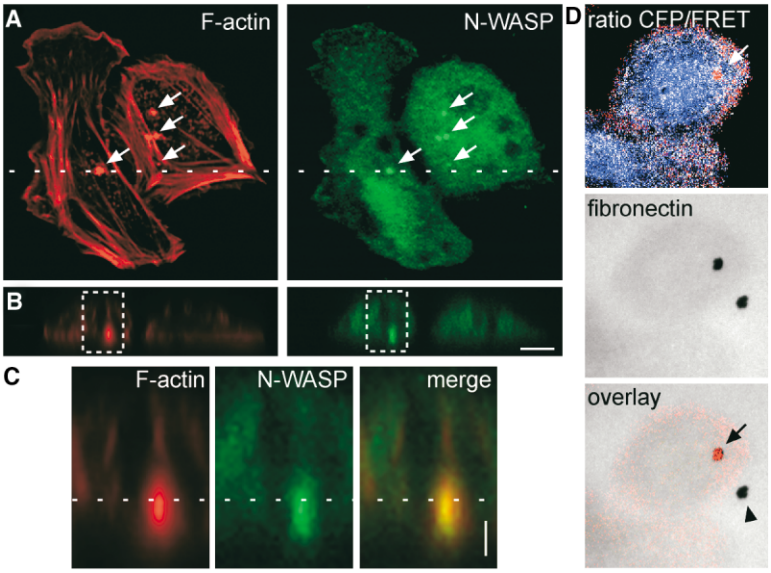

Figure 3. F-Actin and N-WASP Are Enriched in Invadopodia

(A) MTLn3 cells plated on fibronectin coated glass-cover dishes were immunoflurescence stained for F-actin (red) and N-WASP (green). Invadopodia showed a punctuated F-actin and N-WASP staining (arrows).

(B) Z projection of the region indicated by the dashed line in (A) shows that F-actin and N-WASP were present through the whole invadopod (scale bar 10 μm).

(C) Magnification of the boxed area marked in (B) (scale bar 2 μm). The dotted line indicates the cell-matrix surface.

(D) N-WASP is activated in extending invadopodia. The images show the N-WASP activity in MTLn3 cells observed by FRET (ratio CFP/FRET), the Alexa-568 conjugated fibronectin fluorescence, and an overlay of the fibronectin matrix with the N-WASP activity profile. Locations of invadopodia are indicated by black holes in the fibronectin matrix due to ECM degradation. N-WASP activity was observed right at the point of origin of active invadopodia (arrow). The spot outside the cell (arrow head) indicates a spot of a former but now inactive invadopod.

direction of movement (Figure 2A), an area of intense Arp2/3-dependent actin nucleation activity [10]. In order to determine the kinetics of N-WASP activation in epidermal growth factor (EGF)-responding carcinoma cells by FRET, we used the ability of MTLn3 cells to extend lamellipodia with a precise time course in response to uniform addition of EGF [10]. To exclude possible artifacts caused by overexpression of the biosensor, e.g., a misdistribution of the biosensor or disassembly of certain actin structures [11], we established an MTLn3 cell line that stably expresses N-WASP-BS at physiological levels (Figure 1E). The distribution of the N-WASP-BS in these cells was similar to endogenous N-WASP visualized by immunofluorescence staining (see Figure S4). To synchronize the MTLn3 cells, we serum starved them for 3 hr and stimulated them with 5 nM EGF at 37°C [12]. MTLn3 cells were fixed at various time points after simulation and the activity profile of the N-WASP-BS was determined as described above. The results demonstrate an increase of N-WASP activity in EGF stimulated lamellipodia at the leading edge (Figure 2B). This activity peaked at 40 s after stimulation and then returned to prestimulation levels (Figure 2C).

In contrast, previous studies in *Drosophila* S2 by RNAi depletion [13] and in fibroblast of N-WASP knockout mice [14] indicated that N-WASP is not necessary for lamellipodia formation due to an unchanged phenotype after N-WASP downregulation. However, we observed a well temporally regulated lamellipodial N-WASP activity in MTLn3 carcinoma cells in response to growth factor stimulation not detected by standard motility assays. The fact that N-WASP activity seems to be not necessary for the lamellipodia formation [13, 14] but corresponds with the first actin polymerization transient observed in response to EGF [10] suggests that N-WASP is involved in signal sensing toward the chemoattractant.

To investigate this further, we visualized other protrusive events associated with carcinoma cell motility. In addition to the ability to extend lamellipodia and move toward a chemoattractant like EGF, invasive cancer cells can also form actin filament-containing membrane protrusions called invadopodia that extend into extracellular matrix (ECM) and function in matrix degradation, signal sensing, and invasive cell motility [15]. Since N-WASP has been implicated in the formation of invasive membrane protrusions [16], we next examined if N-WASP is also involved in invadopodium formation. Invadopodia were visualized by culturing the cells on a fibronectin matrix coated on crosslinked gelatin films and showed an enrichment of F-actin and N-WASP throughout invadopodia (Figures 3A–3C). When cultured on an approximately 3 μm thick Alexa-568-labeled fibronectin matrix, MTLn3 cells produced dark holes of ECM degradation against a background of bright fluorescent matrix by degrading the matrix in association with invadopodia (Figure 3D). N-WASP activity determined by FRET was colocalized with invodopodia (Figures 3D and S5). This is the first direct evidence that actin polymerization mediated by the N-WASP-Arp2/3 pathway is involved in invadopod formation.

The next question was where in invadopodia was N-WASP activity occurring. Invodopodia extend into the ECM in the z direction. To analyze the location of N-WASP activity in invodopodia (shown in red), we performed 3D FRET measurements (Figure 4A). To improve the image quality and reduce out-of-focus fluorescence signal, we deconvolved the 3D stack of images before performing the FRET analysis. Four different invadopodia in different stages are shown in the z projection (Figures 4A1–4A4). Although N-WASP was present throughout these invadopodia as observed by the YFP-fluorescence of the biosensor (data not shown), the N-WASP activation profile along the invadopodia, measured over the total invadopod width, showed that active N-WASP was only localized at the base. In addition, in new invadopodia with a length shorter than 2 μm (Fig-

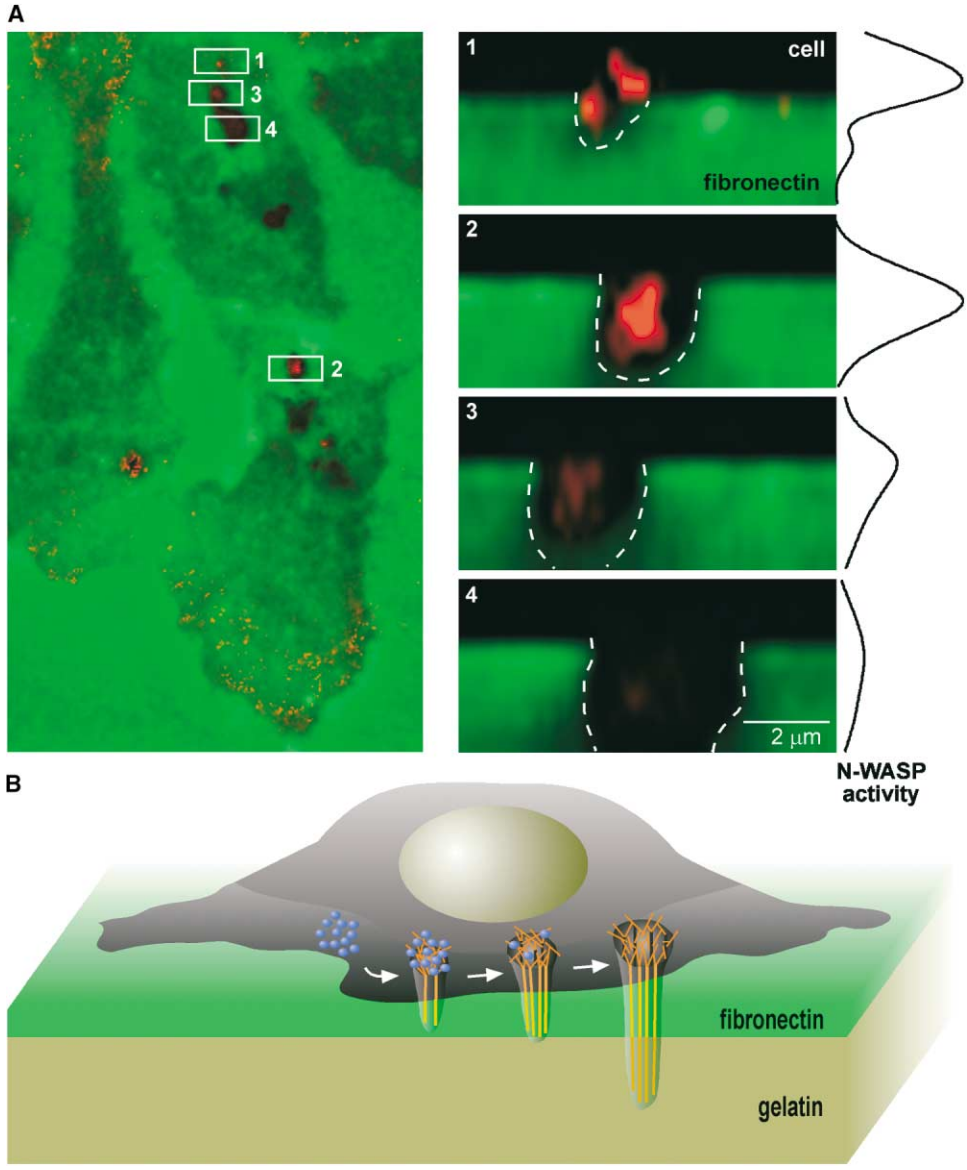

Figure 4. N-WASP Is Activated at the Base of Invadopodia

(A) For a 3D reconstruction of invadopodia we took FRET images every 0.5 μm starting at 2.5 μm below to 1.5 μm above the cell-fibronectin contact surface and deconvolved the z stacks. The left panel shows an xy plot of the stack indicating different invadopodia. N-WASP activity is shown in red. In the right panel, z stacks of four invadopodia, shown in the boxes in the left image, at different stages of extension are shown (1–4). Invadopodia are visible as black holes in the Alexa-568 labeled fibronectin matrix (green) and are indicated by white dashed lines. For clarity, out of focus sections of the fibronectin images are not shown. Invadopodia extending through the fibronectin layer into the non fluorescent gelatin layer appear as a channel in the 3D z projection. At the right side the N-WASP activity profile is plotted versus invadopodium length for each panel. While the acceptor fluorescence and distribution of N-WASP along invodopodia was uniform (data not shown), N-WASP activity was detectable just at the base. The N-WASP activity was significantly higher in new (1 and 2) than in old (3 and 4) invadopodia.

(B) Hypothesis for the function of N-WASP activity in invadopodia. The first step to form invadopodia would be to generate a localized dentritic nucleation mediated by the N-WASP/Arp2/3 pathway. Blue spheres indicate N-WASP activity. For simplicity, actin filaments are drawn as straight lines (orange). N-WASP independent elongation of newly nucleated filaments would push the membrane forward into the ECM. Invadopodium extension is now driven by elongation of these filaments rather than requiring additional nucleation. Thus, the longer the invodopdia extend the lower the N-WASP activity required as observed.

ures 4A1 and 4A2), a higher N-WASP activity was observed than in longer, older invadopodia (Figures 4A3 and 4A4).

These data suggest that N-WASP plays a role in initiation of invadopodia where N-WASP activity and the activity of its downstream effector, the Arp2/3 complex, is constrained to the base. This supports previous findings where N-WASP was implicated in the formation of filopodia, similarly shaped tubular protrusions [4]. While it is possible that Arp2/3 complex can be activated

throughout the invadopod resulting from some other activators, our results support the model proposed for filopodium protrusion by convergent elongation of filaments originating from Arp2/3 complex constrained to the base of filopodia [17]. Our biosensor results are the first to localize N-WASP activity in the basal region of tubular protrusions, suggesting that Arp2/3 activity is localized only to the base and that filament elongation of the protrusion does not involve nucleation of filaments within the protrusion itself. Thus, the first step to initiate invadopodia would be to generate localized dendritic nucleation at the ventral surface by N-WASP activation of the Arp2/3 complex (see Figure 4B). The convergent elongation of newly nucleated filaments supported by Ena/Vasp family proteins [18, 19] or Diaphanous-related formin 3 (Drf3) [20] as suggested for filopodia would push the plasma membrane forward into the ECM. If the force produced by elongation of existing filaments is sufficient to push out the membrane, the N-WASP activity could decrease without affecting further elongation. At this point invadopodium growth would rely upon elongation rather than nucleation. The fact that N-WASP activity is also seen throughout the leading edge of lamellipodia (Figure 2) suggests that the decision to convert the geometry of pushing force of the elongating filaments of the dendritic network from a lamellipodial to a filopodial shape occurs at a step independent of the activation of N-WASP alone. Invadopodium formation greatly enhances the invasion of carcinoma cells [21]. N-WASP has been shown to potentiate invasion [16], and our biosensor results suggest a mechanism for the involvement of N-WASP in invadopodium-mediated invasion. Together, these observations emphasize N-WASP as a target for therapies directed at inhibiting the invasion of carcinomas.

For the first time we measured and imaged directly N-WASP activity in vivo by using FRET microscopy and observed that the ubiquitous N-WASP plays a general role in actin nucleation processes. N-WASP is involved in the cytoskeleton reorganization of lamellipodia of migrating carcinoma cells as well as the initiation of invadopodia. N-WASP can be activated by many upstream factors, including Cdc42, PIP2, or phosphorylation, and it is likely that different cell responses are regulated by different upstream activators. To understand the different functions of N-WASP in each of these pathways, e.g., the formation of invadopodia, lamellipodia, filopodia, etc., it is important to identify the upstream factors regulating N-WASP in each of these different locations, something that the biosensor is well suited to investigate in vivo.

Supplemental Data

Supplemental Data including Experimental Procedures and five figures are available at http://www.current-biology.com/cgi/content/full/14/8/697/DC1/.

Acknowledgments

We thank M. Way (Cancer Research UK, London, UK) for his generous gift of the rat GFP-N-WASP plasmid and M. Cammer (Analytical Imaging Facility, AECOM) for his help with the confocal microscopy. This work was supported by grants from the National Institutes of Health to J.C. (38511) and R.H.S.

Received: December 5, 2003
Revised: February 2, 2004
Accepted: February 27, 2004
Published: April 20, 2004

References

1. Pollard, T.D., and Borisy, G.G. (2003). Cellular motility driven by assembly and disassembly of actin filaments. Cell *112*, 453–465.
2. Pollard, T.D., Blanchoin, L., and Mullins, R.D. (2000). Molecular mechanisms controlling actin filament dynamics in nonmuscle cells. Annu. Rev. Biophys. Biomol. Struct. *29*, 545–576.
3. Takenawa, T., and Miki, H. (2001). WASP and WAVE family proteins: key molecules for rapid rearrangement of cortical actin filaments and cell movement. J. Cell Sci. *114*, 1801–1809.
4. Miki, H., and Takenawa, T. (2003). Regulation of actin dynamics by WASP family proteins. J. Biochem. (Tokyo) *134*, 309–313.
5. Rohatgi, R., Ho, H.Y., and Kirschner, M.W. (2000). Mechanism of N-WASP activation by CDC42 and phosphatidylinositol *4*, 5-bisphosphate. J. Cell Biol. *150*, 1299–1310.
6. Kim, A.S., Kakalis, L.T., Abdul-Manan, N., Liu, G.A., and Rosen, M.K. (2000). Autoinhibition and activation mechanisms of the Wiskott-Aldrich syndrome protein. Nature *404*, 151–158.
7. Fukuoka, M., Suetsugu, S., Miki, H., Fukami, K., Endo, T., and Takenawa, T. (2001). A novel neural Wiskott-Aldrich syndrome protein (N-WASP) binding protein, WISH, induces Arp2/3 complex activation independent of Cdc42. J. Cell Biol. *152*, 471–482.
8. Carlier, M.F., Nioche, P., Broutin-L'Hermite, I., Boujemaa, R., Le Clainche, C., Egile, C., Garbay, C., Ducruix, A., Sansonetti, P., and Pantaloni, D. (2000). GRB2 links signaling to actin assembly by enhancing interaction of neural Wiskott-Aldrich syndrome protein (N-WASp) with actin-related protein (ARP2/3) complex. J. Biol. Chem. *275*, 21946–21952.
9. Higgs, H.N., and Pollard, T.D. (2000). Activation by Cdc42 and PIP(2) of Wiskott-Aldrich syndrome protein (WASp) stimulates actin nucleation by Arp2/3 complex. J. Cell Biol. *150*, 1311–1320.
10. Chan, A.Y., Raft, S., Bailly, M., Wyckoff, J.B., Segall, J.E., and Condeelis, J.S. (1998). EGF stimulates an increase in actin nucleation and filament number at the leading edge of the lamellipod in mammary adenocarcinoma cells. J. Cell Sci. *111*, 199–211.
11. Moreau, V., Tatin, F., Varon, C., and Genot, E. (2003). Actin can reorganize into podosomes in aortic endothelial cells, a process controlled by Cdc42 and RhoA. Mol. Cell. Biol. *23*, 6809–6822.
12. Segall, J.E., Tyerech, S., Boselli, L., Masseling, S., Helft, J., Chan, A., Jones, J., and Condeelis, J. (1996). EGF stimulates lamellipod extension in metastatic mammary adenocarcinoma cells by an actin-dependent mechanism. Clin. Exp. Metastasis *14*, 61–72.
13. Rogers, S.L., Wiedemann, U., Stuurman, N., and Vale, R.D. (2003). Molecular requirements for actin-based lamella formation in Drosophila S2 cells. J. Cell Biol. *162*, 1079–1088.
14. Snapper, S.B., Takeshima, F., Anton, I., Liu, C.H., Thomas, S.M., Nguyen, D., Dudley, D., Fraser, H., Purich, D., Lopez-Ilasaca, M., et al. (2001). N-WASP deficiency reveals distinct pathways for cell surface projections and microbial actin-based motility. Nat. Cell Biol. *3*, 897–904.
15. Chen, W.T. (1989). Proteolytic activity of specialized surface protrusions formed at rosette contact sites of transformed cells. J. Exp. Zool. *251*, 167–185.
16. Yamaguchi, H., Miki, H., and Takenawa, T. (2002). Neural Wiskott-Aldrich syndrome protein is involved in hepatocyte growth factor-induced migration, invasion, and tubulogenesis of epithelial cells. Cancer Res. *62*, 2503–2509.
17. Svitkina, T.M., Bulanova, E.A., Chaga, O.Y., Vignjevic, D.M., Kojima, S., Vasiliev, J.M., and Borisy, G.G. (2003). Mechanism of filopodia initiation by reorganization of a dendritic network. J. Cell Biol. *160*, 409–421.
18. Lanier, L.M., Gates, M.A., Witke, W., Menzies, A.S., Wehman, A.M., Macklis, J.D., Kwiatkowski, D., Soriano, P., and Gertler, F.B. (1999). Mena is required for neurulation and commissure formation. Neuron *22*, 313–325.

19. Rottner, K., Behrendt, B., Small, J.V., and Wehland, J. (1999). VASP dynamics during lamellipodia protrusion. Nat. Cell Biol. *1*, 321–322.
20. Peng, J., Wallar, B.J., Flanders, A., Swiatek, P.J., and Alberts, A.S. (2003). Disruption of the Diaphanous-Related Formin Drf1 Gene Encoding mDia1 Reveals a Role for Drf3 as an Effector for Cdc42. Curr. Biol. *13*, 534–545.
21. Chen, W.T., Yeh, Y., and Nakahara, H. (1994). An in vitro cell invasion assay: Determination of cell surface proteolytic activity that degrades extracellular matrix. J. Tissue Cult. Methods *16*, 177–181.